

Optimal Reduced-order Modeling of Bipedal Locomotion

Yu-Ming Chen¹ and Michael Posa¹

Abstract—State-of-the-art approaches to legged locomotion are widely dependent on the use of models like the linear inverted pendulum (LIP) and the spring-loaded inverted pendulum (SLIP), popular because their simplicity enables a wide array of tools for planning, control, and analysis. However, they inevitably limit the ability to execute complex tasks or agile maneuvers. In this work, we aim to automatically synthesize models that remain low-dimensional but retain the capabilities of the high-dimensional system. For example, if one were to restore a small degree of complexity to LIP, SLIP, or a similar model, our approach discovers the form of that additional complexity which optimizes performance. In this paper, we define a class of reduced-order models and provide an algorithm for optimization within this class. To demonstrate our method, we optimize models for walking at a range of speeds and ground inclines, for both a five-link model and the Cassie bipedal robot.

I. INTRODUCTION

Modern legged robots, like the Agility Robotics Cassie, have many degrees of freedom, tens or more actuators and may have passive dynamic elements such as springs and dampers. To manage this complexity, and simplify the process of planning and control design, the community has embraced the use of reduced-order models. Particularly popular are the linear inverted pendulum (LIP) [1], [2], the spring-loaded inverted pendulum (SLIP) [3], and various permutations. The LIP has a long history as a predominant approach in robot walking, and formed the basis of many approaches taken during the DARPA robotics challenge [4], [5], [6]. The SLIP is widely used to explain energy efficient running [7], [8], [9], [10]. These models have been empirically shown to capture the dominant dynamics of the robots in particular tasks, and their simplicity enables solutions to the challenging problems of control and planning design. For example, many of locomotion planning problems can be solved in realtime with the low-dimensional models [11].

The downside, however, is that by forcing robots to act like a low-degree-of-freedom model, these approaches restrict the motion of complex robots and necessarily sacrifices performance. This can result in energetically inefficient motion, or fail to extend to wide range of tasks. For example, the LIP greatly restricts both efficiency and stride length. These limitations have long been acknowledged by the community, resulting in a wide array of extensions that universally rely on human intuition, and are generally in the form of mechanical components (a spring, a damper, a joint, a rigid body with inertia, etc) [12], [13], [14], [15], [16], [17], [18].

¹Yu-Ming Chen and Michael Posa are with the General Robotics, Automation, Sensing and Perception (GRASP) Laboratory, University of Pennsylvania, Philadelphia, PA 19104, USA {ymchen, posa}@seas.upenn.edu

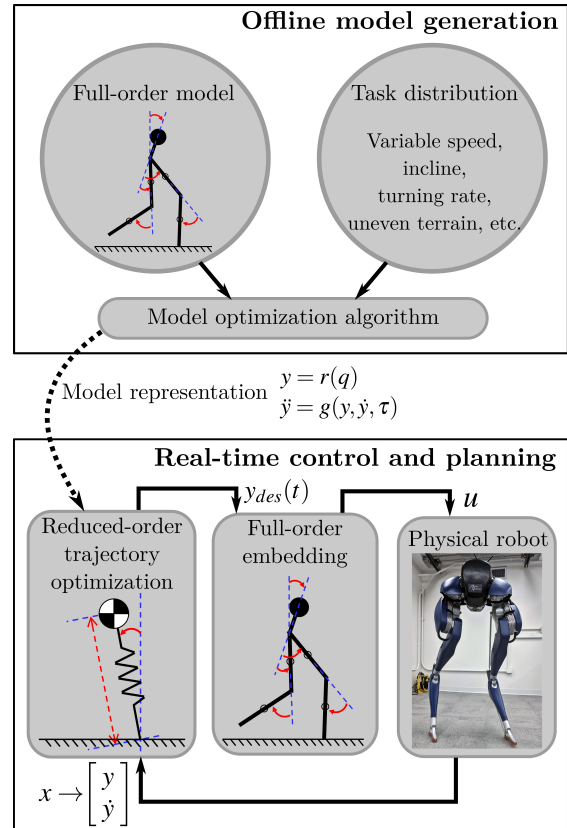


Fig. 1: An outline of the synthesis and deployment of optimal reduced-order models. Offline, given a full-order model and a distribution of tasks, we optimize a new model that is effective over the task space. Online, we generate new plans for the reduced-order model and track these trajectories on the true, full-order system.

The ad hoc nature of these extensions demonstrates that the community implicitly admits both that the simplest models are insufficient, and that it is not known which extensions are most beneficial. Additionally, it has been shown that not all model extensions improve the performance of robots much. For example, allowing center of mass height to vary provides limited aid in the task of balancing [19], [20].

The primary contribution of this paper is an optimization algorithm to automatically synthesize new reduced order models, embedding high-performance capabilities within low-dimensional representations. Given a distribution of tasks, and a nominal full-order model, we propose a bilevel optimization of stochastic gradient descent and trajectory optimization to search within a broad class of simple models.

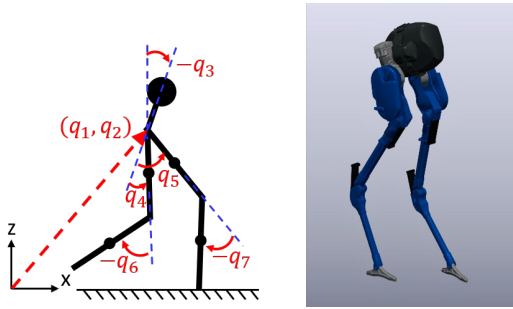


Fig. 3: Examples of full-order models. On the left is a five-link robot. On the right is the 3D Cassie biped, which has five actuators per leg.

Therefore, we use stochastic gradient descent as the outer loop (to trajectory optimization in the inner loop). That is, we sample a set of tasks from the distribution Γ and optimize the averaged sample cost over the model parameters θ .

The full approach to (O) is outlined in Algorithm 1. Starting from an initial parameter seed θ_0 , N tasks are sampled, and the cost for each task is evaluated by solving the corresponding trajectory optimization problem (TO).

To compute each gradient $\nabla_{\theta} [\mathcal{J}_{\gamma_j}(\theta)]$, we adopt an approach based in sequential quadratic programming. We locally approximate (TO) with an equality-constrained quadratic program, only considering the active constraints. Let $\tilde{w}_{\gamma} = w - w_{\gamma}^*$ and $\tilde{\theta} = \theta - \theta^{(i)}$, where w_{γ}^* is the optimal solution of (TO), and $\theta^{(i)}$ is the parameter at the i -th iteration. The approximated quadratic program is

$$\begin{aligned} \mathcal{J}_{\gamma}(\theta) \approx \min_{w_{\gamma}} \quad & \frac{1}{2} \tilde{w}_{\gamma}^T H_{\gamma} \tilde{w}_{\gamma} + b_{\gamma}^T \tilde{w}_{\gamma} + c_{\gamma} \\ \text{s.t.} \quad & F_{\gamma} \tilde{w}_{\gamma} + G_{\gamma} \tilde{\theta} = 0 \end{aligned} \quad (8)$$

Using the Karush-Kuhn-Tucker (KKT) conditions [41], we can derive the following equation for the optimal solution

$$\begin{bmatrix} H_{\gamma} & F_{\gamma}^T \\ F_{\gamma} & 0 \end{bmatrix} \begin{bmatrix} \tilde{w}_{\gamma}^* \\ v_{\gamma}^* \end{bmatrix} = \begin{bmatrix} -b_{\gamma} \\ -G_{\gamma} \tilde{\theta} \end{bmatrix}, \quad (9)$$

where v_{γ}^* is the optimal dual solution. (9) can be further solved, with the solution rewritten as

$$\tilde{w}_{\gamma}^* = Q_{\gamma} \tilde{\theta} + p_{\gamma}, \quad (10)$$

for some $Q_{\gamma} \in \mathbb{R}^{n_w \times n_{\theta}}$ and $p_{\gamma} \in \mathbb{R}^{n_w}$. Since we approximate the original problem around w^* and $\theta^{(i)}$, we know that $\tilde{w}_{\gamma}^* = 0$ if $\tilde{\theta} = 0$; therefore, $p_{\gamma} = 0$. Substituting (10) into (8) and taking the gradient of \mathcal{J}_{γ_j} , we derive

$$\nabla_{\theta} [\mathcal{J}_{\gamma_j}(\theta)] \Big|_{\theta=\theta^{(i)}} = Q_{\gamma_j}^{\top} b_{\gamma_j}. \quad (11)$$

The algorithm is deemed to have converged if the norm of the gradient falls below a specified threshold.

IV. EXAMPLES

We test our algorithm of model optimization with two robots: a five-link planar robot and the three dimensional Cassie biped (Fig. 3). For all examples, the motions of the

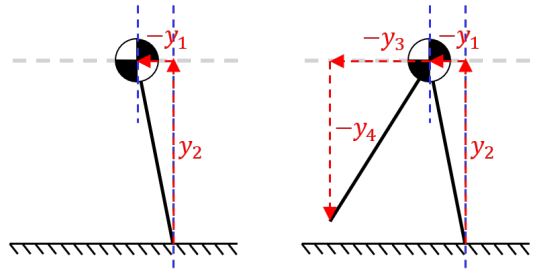


Fig. 4: Two initial reduced-order models with generalized positions. On the left is the standard LIP; on the right is an LIP with an actuated swing foot.

optimized models are shown in the accompanying video². Examples were generated using the Drake software toolbox [42] and source code is freely available².

The planar robot consists of five links with non-zero mass and inertia, and four actuated joints with torque saturation. The thighs and shanks are of mass 2.5 kg and length 0.5 m. The weight of the torso is 10 kg and the length is 0.3 m. The robot has point feet, and the contacts between feet and ground are perfectly inelastic.

The Cassie has stiff rotational springs in the knees and ankles. Here, however, we simplify the model by treating these springs as infinitely stiff; this simplification is necessary for the coarse integration steps used in trajectory optimization, and has been used successfully with Cassie [43]. The legs also contain two four-bar linkages, which we model with a fixed-distance constraint and corresponding constraint force. There are five motors on each leg. Three located at the hip, one at the knee, and one at the toe.

The hybrid equations of motion of either robot are written

$$\begin{cases} \dot{x} = f(x, u), & x^- \notin S \\ x^+ = \Delta(x^-, \Lambda), & x^- \in S \end{cases} \quad (12)$$

where x^- and x^+ are pre- and post-impact state, Λ is the impulse of swing foot touchdown, Δ is the discrete mapping of the touchdown event, and S is the surface in the state space where the event must occur.

We assume the robot walks with instantaneous change of support. That is, the robot transitions from right support to left support instantaneously, and vice versa. Therefore, the phase sequence cycles through a single support phase. For the examples here, we consider only half-gait periodic motion, and so include right-left leg alternation in the impact map Δ .

A. Initial reduced-order models

To demonstrate the algorithm, we optimized two reduced-order models for each robot. For the five-link robot, we initialize the first model with LIP and the second model with LIP plus an actuated point-mass swing foot (Fig. 4). The generalized positions y for both models are shown in Fig. 4. For reference, the equations of motion of the LIP

² <https://sites.google.com/view/ymchen/research/optimal-rom>

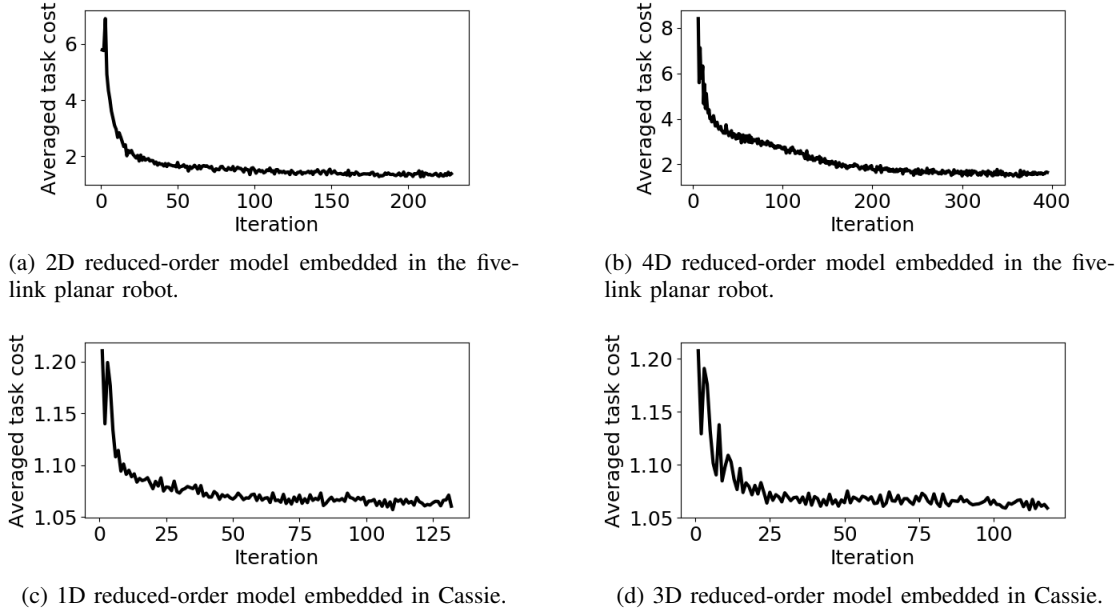


Fig. 5: The averaged cost of the sampled tasks over iterations. Costs are normalized by the cost associated with the full-order model (a lower bound on any reduced-order model). The costs at iteration 1 represent the averaged costs for the robots with the embedded initial reduced-order models, e.g. LIP. Note that the empirical average does not strictly decrease, as tasks are randomly sampled and are of varying difficulty.

model with a point-mass swing foot are

$$\ddot{y} = \begin{bmatrix} \ddot{y}_1 \\ \ddot{y}_2 \\ \ddot{y}_3 \\ \ddot{y}_4 \end{bmatrix} = \begin{bmatrix} c_g \cdot y_1/y_2 \\ 0 \\ 0 \\ 0 \end{bmatrix} + \begin{bmatrix} 0 & 0 \\ 0 & 0 \\ 1 & 0 \\ 0 & 1 \end{bmatrix} \begin{bmatrix} \tau_1 \\ \tau_2 \end{bmatrix}, \quad (13)$$

where c_g is the gravitational acceleration. For the LIP model, the dynamics are given in the first two rows of (13).

Similarly, we initialize the models for Cassie with the two models mentioned above except that we reduce the model dimensions by removing y_1 in Fig. 4 from both models. These models represent a point-mass body with/without a swing foot, where the body has a constant speed in the vertical direction. We choose this initialization because the solver struggles to find a good optimal solution to (TO) when the LIP constraint is imposed.

B. Five-link planar robot

The generalized position q is 7 dimensional where the first 3 elements are the floating-base joint. Recall that the contact constraint with the ground is solved implicitly.

We choose a rich feature set ϕ_e that includes the COM position with respect to the stance foot, the swing foot position with respect to the center of mass, the hip position (q_1, q_2) , and all quadratic combinations of the elements in $\{1, \cos(q_3), \sin(q_3), \dots, \cos(q_7), \sin(q_7)\}$.

For the 2D model, the feature set ϕ_d includes $c_g \cdot y_1/y_2$, and all quadratic combinations of the elements in $\{1, y_1, y_2, \dot{y}_1, \dot{y}_2\}$. For the 4D model, the feature set ϕ_2 is constructed in a similar way. Note that these feature vectors were chosen to explicitly include elements of the LIP and

the LIP with a swing foot, but also include a diverse set of additional terms. Initial parameters θ can be easily chosen to match the LIP-based initial models.

We choose the tasks γ to include walking with different speeds between 0.27 and 0.54 m/s and on ground inclines between -0.08 and 0.08 radians. The cost h_γ is the sum of weighted norm of generalized velocity \dot{q} , input of the robot u and input of the reduced-order model τ . We include τ in the cost to regularize the input to the reduced-order model, and to correlate it with cost on the original model.

Fig. 5a and 5b show results from optimization, where the empirical average cost decreases rapidly during the process. The optimized model is capable of expressing lower cost and more natural motion² than the LIP, better leveraging the natural dynamics of the five-link model.

C. Cassie

The generalized position q of Cassie is 19 dimensional where the first 7 elements are the floating-base joint (translation and rotation expressed via quaternion). The feature sets ϕ_e and ϕ_d are constructed in a similar way to that of the five-link robot example. We pick the tasks γ to be walking with different speeds between 0.25 and 0.75 m/s and on different ground inclines between -0.08 and 0.08 radians.

Results, showing average cost per iteration, are shown in Fig. 5c and 5d. As with the simpler example, reduced-order model optimization maintains model simplicity but improves performance. However, the costs with the initial models are much lower than those in the five-link robot example. The reason are that there are fewer constraints from the reduced-order models, and that Cassie has more joints and degree of

freedom than the five-link robot. Furthermore, we note that the final, optimized model, unlike its classical counterpart, does not map easily to a simple, physical model. While this limits our ability to attach physical meaning to y and τ , we believe this to be a necessary sacrifice to improve performance beyond that of hand-designed approaches.

V. PLANNING WITH REDUCED-ORDER MODELS

As shown in Fig. 1, given an optimal model μ^* , we plan in the reduced-order space. As an example, we formulate a trajectory optimization problem to walk l meters in n_s strides. Since the reduced-order model only captures the continuous dynamics, and perfect embedding of a reduced-order hybrid model is often impossible, we mix the reduced-order model with the discrete dynamics from the full-order model. This approach results in a low-dimensional trajectory optimization problem, a search for $y_j(t)$ and $\tau_j(t)$, with additional decision variables $x_{-,j}, x_{+,j}$, representing the pre- and post-impact full-order states. The index $j = 1, \dots, n_s$ refers to the j th stride. The additional constraints relating these full-order states to the impact mapping and the reduced order model are

$$\begin{aligned} y_j(t_j) &= r(q_{-,j}; \theta_e), & \dot{y}_j(t_j) &= \frac{\partial r(q_{-,j}; \theta_e)}{\partial q_{-,j}} \dot{q}_{-,j}, \\ y_{j+1}(t_j) &= r(q_{+,j}; \theta_e), & \dot{y}_{j+1}(t_j) &= \frac{\partial r(q_{+,j}; \theta_e)}{\partial q_{+,j}} \dot{q}_{+,j}, \\ & \text{and} & C_{\text{hybrid}}(x_{-,j}, x_{+,j}, \Lambda_j) &\leq 0, \end{aligned}$$

where t_j 's are the impact times (ending the j th stride), C_{hybrid} represents the hybrid guard S and the impact mapping Δ without left-right leg alternation. Costs are nominally expressed in terms of $[y^\top, \dot{y}^\top]^\top$ and τ , though the pre- and post-impact full-order states can also be used to represent goal locations. This formulation preserves an exact representation of the hybrid dynamics, but results in a significantly reduced optimization problem that can be used for real-time planning.

We tested the planning algorithm with the optimized 4D model embedded in the five-link robot. The distance l varies from 0.2 to 6 meters with stride numbers n_s between 1 to 10. To plan a single step, the average runtime was 240 ms, on a computer with Intel i7-8750H processor, without optimizing code for efficiency. Similar code required tens of seconds for the full-order model. We note that including the full-order state impact states roughly doubles the computation time, as planning purely with the reduced-order model, without impacts, takes only 110 ms.

Fig. 6 visualizes the pre-impact states in the case where the robot walks two meters with four strides, connected by the hybrid events and continuous low-dimensional trajectories $y_j(t)$. We were able to retrieve $q(t)$ from $y_j(t)$ through inverse kinematics, meaning that the optimal trajectories $y_j(t)$ are feasible for the robot. The resulting motion, shown in the accompanying video², looks smooth and is qualitatively more efficient than the gait that the original model (LIP with a foot) would generate.

We note that reduced-order model trajectories for walking are necessarily hybrid, except for zero-impact motions.

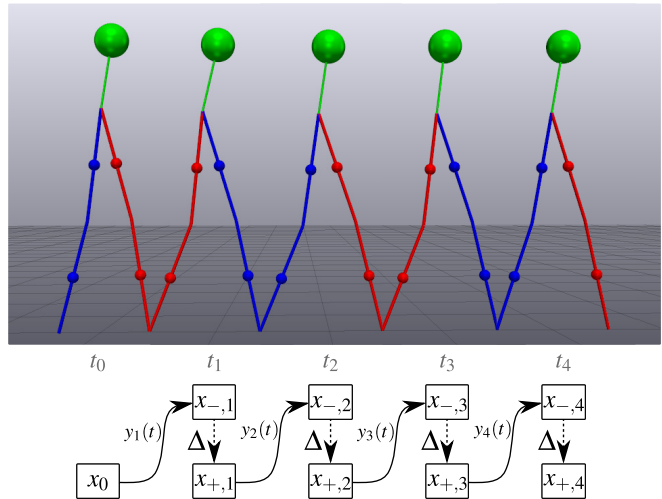


Fig. 6: Given a task of covering two meters in four steps, we rapidly plan a trajectory for the reduced-order model. The high-dimensional model is used to capture the hybrid event, at stepping, as illustrated in the cartoon.

Therefore, traditional approaches to reduced-order planning and embedding must also grapple with approximations of the impact event.

The example above demonstrates that the mixed model planner greatly reduces planning speed, and that the optimized reduced-order models can be used to achieve tasks in full-order space.

VI. DISCUSSION

We present a novel method for automatically generating reduced-order models for legged locomotion, a step toward uncovering which aspects of the dynamics are necessary for tasks performance. This approach is demonstrated over an array of tasks on both a simple, planar robot and a 3D model of the Cassie. We also present an algorithm, suitable for real-time use, for planning reduced-order trajectories.

While there is no guarantee that the motions planned in Section V are feasible for the full model, we observe, empirically, that embeddings do seem to exist, and also note that classical models like LIP also provide no guarantees. One direction for future work, for both LIP and the optimized models, is to generate constraints for reduced-order planning that guarantee feasibility on the original system.

Other future work will continue to develop and deploy reduced-order models, with an immediate goal of tracking and executing the planned motions on the physical Cassie robot using operational space control (e.g. [34]). In Section V, we note that the planner must still use the full-order model for the discrete mapping; future work will explore optimization of hybrid reduced-order model. Since impact maps are fully autonomous, it is not possible to find a perfect, low-order reduction. This necessitates the need for approximate hybrid models, where we will leverage existing notions of hybrid distance [44]. Lastly, we would like to

increase the tasks space and explore alternative function bases to evaluate the quality of different resulting models.

REFERENCES

- [1] S. Kajita and K. Tani, "Study of dynamic biped locomotion on rugged terrain-derivation and application of the linear inverted pendulum mode," vol. 2, pp. 1405–1411, IEEE International Conference on Robotics and Automation (ICRA), 1991.
- [2] S. Kajita, F. Kanehiro, K. Kaneko, K. Yokoi, and H. Hirukawa, "The 3D linear inverted pendulum mode: a simple modeling for a biped walking pattern generation," pp. 239–246, IEEE International Conference on Intelligent Robots and Systems (IROS), 2001.
- [3] R. Blickhan, "The spring-mass model for running and hopping," *Journal of biomechanics*, vol. 22, no. 11-12, pp. 1217–1227, 1989.
- [4] S. Feng, E. Whitman, X. Xinjilefu, and C. G. Atkeson, "Optimization-based Full Body Control for the DARPA Robotics Challenge," *Journal of Field Robotics*, vol. 32, no. 2, pp. 293–312, 2015.
- [5] T. Koolen, J. Smith, G. Thomas, S. Bertrand, J. Carff, N. Mertins, D. Stephen, P. Abeles, J. Engelsberger, S. McCrory, J. van Egmond, M. Griffioen, M. Floyd, S. Kobus, N. Manor, S. Alsheikh, D. Duran, L. Bunch, E. Morphis, L. Colasanto, K.-L. H. Hoang, B. Layton, P. Neuhaus, M. Johnson, and J. Pratt, "Summary of Team IHMC's Virtual Robotics Challenge Entry," in *Proceedings of the IEEE-RAS International Conference on Humanoid Robots*, (Atlanta, GA), oct 2013.
- [6] S. Kuindersma, R. Deits, M. Fallon, A. Valenzuela, H. Dai, F. Permenter, T. Koolen, P. Marion, and R. Tedrake, "Optimization-based locomotion planning, estimation, and control design for Atlas," *Autonomous Robots*, vol. 40, no. 3, pp. 429–455, 2016.
- [7] M. Hutter, C. D. Remy, M. A. Höpflinger, and R. Siegwart, "Slip running with an articulated robotic leg," in *2010 IEEE/RSJ International Conference on Intelligent Robots and Systems*, pp. 4934–4939, IEEE, 2010.
- [8] I. Poulakakis and J. W. Grizzle, "The spring loaded inverted pendulum as the hybrid zero dynamics of an asymmetric hopper," *IEEE Transactions on Automatic Control*, vol. 54, no. 8, pp. 1779–1793, 2009.
- [9] C. Hubicki, A. Abate, P. Clary, S. Rezazadeh, M. Jones, A. Peekema, J. Van Why, R. Domres, A. Wu, W. Martin, et al., "Walking and running with passive compliance," *IEEE ROBOTICS AND AUTOMATION MAGAZINE*, vol. 1, 2016.
- [10] W. C. Martin, A. Wu, and H. Geyer, "Experimental evaluation of deadbeat running on the atrias biped," *IEEE Robotics and Automation Letters*, vol. 2, no. 2, pp. 1085–1092, 2017.
- [11] T. Appgar, P. Clary, K. Green, A. Fern, and J. W. Hurst, "Fast online trajectory optimization for the bipedal robot cassie.," in *Robotics: Science and Systems*, 2018.
- [12] J. Pratt, P. Dilworth, and G. Pratt, "Virtual model control of a bipedal walking robot," in *Proceedings of International Conference on Robotics and Automation*, vol. 1, pp. 193–198, IEEE, 1997.
- [13] R. Sellaouti, O. Stasse, S. Kajita, K. Yokoi, and A. Kheddar, "Faster and smoother walking of humanoid hrp-2 with passive toe joints," in *2006 IEEE/RSJ International Conference on Intelligent Robots and Systems*, pp. 4909–4914, IEEE, 2006.
- [14] M. Hutter, C. D. Remy, M. A. Hoepflinger, and R. Siegwart, "Scarleth: Design and control of a planar running robot," in *2011 IEEE/RSJ International Conference on Intelligent Robots and Systems*, pp. 562–567, IEEE, 2011.
- [15] G. Garofalo, C. Ott, and A. Albu-Schäffer, "Walking control of fully actuated robots based on the bipedal slip model," in *2012 IEEE International Conference on Robotics and Automation*, pp. 1456–1463, IEEE, 2012.
- [16] S. Faraji and A. J. Ijspeert, "3lp: A linear 3d-walking model including torso and swing dynamics," *the international journal of robotics research*, vol. 36, no. 4, pp. 436–455, 2017.
- [17] T. Koolen, T. De Boer, J. Rebula, A. Goswami, and J. Pratt, "Capturability-based analysis and control of legged locomotion, part 1: Theory and application to three simple gait models," *The International Journal of Robotics Research*, vol. 31, no. 9, pp. 1094–1113, 2012.
- [18] T. Libby, A. M. Johnson, E. Chang-Siu, R. J. Full, and D. E. Koditschek, "Comparative design, scaling, and control of appendages for inertial reorientation," *IEEE Transactions on Robotics*, vol. 32, no. 6, pp. 1380–1398, 2016.
- [19] M. Posa, T. Koolen, and R. Tedrake, "Balancing and Step Recovery Capturability via Sums-of-Squares Optimization," in *Robotics: Science and Systems*, 2017.
- [20] T. Koolen, M. Posa, and R. Tedrake, "Balance control using center of mass height variation: limitations imposed by unilateral contact," in *Humanoid Robots (Humanoids), 2016 IEEE-RAS 16th International Conference on*, pp. 8–15, IEEE, 2016.
- [21] R. J. Full and D. E. Koditschek, "Templates and anchors: neuromechanical hypotheses of legged locomotion on land," *The Journal of Experimental Biology*, vol. 202, pp. 3325–3332, 1999.
- [22] U. Saranlı, M. Buehler, and D. E. Koditschek, "RHex: A Simple and Highly Mobile Hexapod Robot," *The International Journal of Robotics Research*, vol. 20, pp. 616–631, jul 2001.
- [23] M. H. Raibert, H. B. Brown, and M. Chepponis, "Experiments in Balance with a 3D One-Legged Hopping Machine," *The International Journal of Robotics Research*, vol. 3, pp. 75–92, jun 1984.
- [24] M. Garcia, A. Chatterjee, A. Ruina, and M. Coleman, "The Simplest Walking Model: Stability, Complexity, and Scaling," *Journal of Biomechanical Engineering*, vol. 120, p. 281, apr 1998.
- [25] A. L. Schwab and M. Wisse, "BASIN OF ATTRACTION OF THE SIMPLEST WALKING MODEL," in *ASME 2001 Design Engineering Technical Conferences and Computers and Information in Engineering Conference*, 2001.
- [26] R. D. Gregg, A. K. Tilton, S. Candido, T. Bretl, and M. W. Spong, "Control and planning of 3-D dynamic walking with asymptotically stable gait primitives," *IEEE Transactions on Robotics*, vol. 28, no. 6, pp. 1415–1423, 2012.
- [27] P. A. Bhounsule, J. Cortell, A. Grewal, B. Hendriksen, J. G. D. Karszen, C. Paul, and A. Ruina, "Low-bandwidth reflex-based control for lower power walking: 65 km on a single battery charge," *The International Journal of Robotics Research*, vol. 33, pp. 1305–1321, sep 2014.
- [28] A. Hereid, S. Kolathaya, M. S. Jones, J. Van Why, J. W. Hurst, and A. D. Ames, "Dynamic multi-domain bipedal walking with atrias through SLIP based human-inspired control," in *Proceedings of the 17th international conference on Hybrid systems: computation and control - HSCC '14*, (New York, New York, USA), pp. 263–272, ACM Press, 2014.
- [29] K. Byl and R. Tedrake, "Metastable Walking Machines," *The International Journal of Robotics Research*, vol. 28, pp. 1040–1064, aug 2009.
- [30] C. Oguz Saglam and K. Byl, "Robust Policies via Meshing for Metastable Rough Terrain Walking," in *Robotics: Science and Systems*, 2014.
- [31] M. Kelly and A. Ruina, "Non-linear robust control for inverted-pendulum 2D walking," in *2015 IEEE International Conference on Robotics and Automation (ICRA)*, pp. 4353–4358, IEEE, may 2015.
- [32] T. Koolen, T. de Boer, J. Rebula, A. Goswami, and J. Pratt, "Capturability-based analysis and control of legged locomotion, Part 1: Theory and application to three simple gait models," *The International Journal of Robotics Research*, vol. 31, no. 9, pp. 1094–1113, 2012.
- [33] J. Pratt, J. Carff, S. Drakunov, and A. Goswami, "Capture point: A step toward humanoid push recovery," in *2006 6th IEEE-RAS international conference on humanoid robots*, pp. 200–207, IEEE, 2006.
- [34] P. M. Wensing and D. E. Orin, "Generation of dynamic humanoid behaviors through task-space control with conic optimization," in *2013 IEEE International Conference on Robotics and Automation*, pp. 3103–3109, IEEE, may 2013.
- [35] T. Suzuki and K. Ohnishi, "Trajectory Planning of Biped Robot with Two Kinds of Inverted Pendulums," in *2006 12th International Power Electronics and Motion Control Conference*, pp. 396–401, IEEE, aug 2006.
- [36] J. T. Betts, *Practical Methods for Optimal Control Using Nonlinear Programming*. SIAM Advances in Design and Control, Society for Industrial and Applied Mathematics, 2001.
- [37] M. Posa, C. Cantu, and R. Tedrake, "A Direct Method for Trajectory Optimization of Rigid Bodies Through Contact," *The International Journal of Robotics Research*, vol. 33, pp. 69–81, jan 2013.
- [38] M. Posa, S. Kuindersma, and R. Tedrake, "Optimization and stabilization of trajectories for constrained dynamical systems," in *2016 IEEE International Conference on Robotics and Automation*, vol. 2016-June, (Stockholm, Sweden), pp. 1366–1373, may 2016.
- [39] P. E. Gill, W. Murray, and M. A. Saunders, "[SNOPT]: An {SQP} Algorithm for Large-Scale Constrained Optimization," *SIAM Review*, vol. 47, no. 1, pp. 99–131, 2005.

- [40] C. R. Hargraves and S. W. Paris, "Direct Trajectory Optimization using Nonlinear Programming and Collocation," *J Guidance*, vol. 10, no. 4, pp. 338–342, 1987.
- [41] H. W. Kuhn and A. W. Tucker, "Nonlinear programming," in *Proceedings of the Second Berkeley Symposium on Mathematical Statistics and Probability*, (Berkeley, Calif.), pp. 481–492, University of California Press, 1951.
- [42] R. Tedrake and the Drake Team Development, "Drake: A planning, control, and analysis toolbox for nonlinear dynamical systems," 2016.
- [43] A. Hereid, O. Harib, R. Hartley, Y. Gong, and J. W. Grizzle, "Rapid bipedal gait design using c-frost with illustration on a cassie-series robot," *arXiv preprint arXiv:1807.06614*, 2018.
- [44] S. A. Burden, H. Gonzalez, R. Vasudevan, R. Bajcsy, and S. S. Sastry, "Metatrization and Simulation of Controlled Hybrid Systems," *IEEE Transactions on Automatic Control*, vol. 60, pp. 2307–2320, sep 2015.